Performance Verification of 3D Image Correlation Using Digital High-Speed Cameras

T. Schmidt, J. Tyson, Trilion Quality Systems, 200 Barr Harbor Dr. Suite 400, West Conshohocken, PA 19428
D.M. Revilock, Jr., S. Padula II, J.M. Pereira, M. Melis, NASA Glenn, 21000 Brookpark Rd, Cleveland, OH 44135
K. Lyle, NASA Langley Research Center, 12 West Bush Road, MS 495, Hampton, VA 23681

ABSTRACT

3D image correlation photogrammetry using Phantom v7 digital high-speed cameras is being used extensively to verify and iterate finite element models of ballistic impact events for the NASA Return to Flight program. In order to ensure the accuracy of the dynamic displacement and strain data measured with the 3D image correlation system, a series of performance tests was conducted in both field and laboratory conditions, with data acquisition rates from 10,000-27,000 frames per second. Rigid body panel translation results conducted in-situ on a test range matched a calibrated micrometer within 1.09% for 0.1" increments from 0.1 to 1.0 inches, with much greater accuracy for most increments. Dynamic displacements from a bend and release test in a laboratory closely matched those from a laser interferometer, with a worst-case error of 1.27%, and strains from the same test closely matched both strain gauges and calculated values. In addition, dynamic strains reported during critical Return to Flight Orbiter wing leading edge panel impact tests were repeatedly found to match data from strain gauges within the field of view. 3D image correlation using digital high-speed cameras has been shown to be an invaluable tool, now in everyday use for critical ballistic impact investigations. The technique is also broadly applicable for air blast deformation measurements, crash testing, drop testing, high strain rate testing, and other dynamic phenomena.

INTRODUCTION

Most people are probably aware that the root cause of the Columbia tragedy was foam that broke loose from the external tank and impacted the reinforced carbon-carbon (RCC) leading edge on the left wing of the orbiter [1]. The accident investigation segued into extensive ballistic impact testing that is in fact still ongoing at the NASA Glenn Ballistic Impact Research Laboratory, Southwest Research Institute, and other locations. Beyond damage tolerance thresholding, the primary goal is to validate LS-DYNA models in accordance with the Columbia Accident Investigation Board (CAIB) requirement 3.8-2, as detailed in the NASA Return to Flight Implementation Plan [2]. Importantly, the primary validation method for the explicit LS-DYNA models is comparison to dynamic displacements obtained from the ARAMIS 3D image correlation using digital high-speed cameras, typically operating with 256 x 256 pixels at 27,000 frames per second. The image correlation system was used for more than 100 RCC coupon ballistic impact tests at NASA Glenn and more than 25 full-scale leading edge shots at Southwest Research Institute. In addition, it was also used for more than 175 external tank coupon test impact studies as part of the broader impact investigation.

LS-DYNA outputs displacements as a primary quantity, and so does a 3D image correlation system. Therefore, the top priority was to directly validate dynamic displacement data. However, it was also considered worthwhile to evaluate dynamic strain data.

3D image correlation photogrammetry is a full-field displacement and strain measurement tool increasingly used for static and slow rate testing, which has also been applied with pulsed illumination for high speed rotating component evaluation [3]. Sample preparation consists of applying a regular or random high contrast dot pattern to the surface, commonly with spray paint. Thousands of overlapping unique correlation areas known as facets (typically 15 pixels square) are defined across the entire imaging area. The center of each facet is a measurement point that can be thought of as a 3D extensometer. Closely spaced arrays of them form in-plane strain rosettes. The facet centers are tracked, in each successive pair of images, with accuracy up to one hundredth of a pixel. Then, using the principles of photogrammetry, the 3D coordinates of each facet are determined for each picture set. The results are the 3D shape of the component, the 3D displacements, and the in-plane strains. Data can be presented as color plots, movies, section line diagrams, etc, and ASCII exports support further analysis and comparison. Because of similar output, this is an excellent tool for verifying and iterating finite element models; it provides distribution as well as maximum values of displacements and strains. The method is extremely robust. It has wide dynamic range and is not affected by rigid body motions, ambient vibrations, etc. The key feature that is exploited when using high speed cameras is that, simply put, as long as pairs of non-blurred pictures can be captured, 3D coordinates, 3D displacements and the in-plane strains can be measured.

The basic principles of 3D image correlation photogrammetry have been known for about 15 years [4]. The particular 3D image correlation system under investigation, ARAMIS, has been commercially available for about 10 years, and has an installed base of about 225 systems worldwide. Most end users have performed their own in-house validation effort, either before or after purchase. For example, by thoroughly validating the application of the ARAMIS 3D image correlation system for residual stress measurement, Nelson [5] has indirectly confirmed the accuracy of in-plane displacement measurements, including the use of an existing movement correction algorithm to compensate for rigid body motion. The peak displacement values caused by stress relaxation around the 3.175 mm diameter hole within the 10 x 8 mm field of view were a few microns, with high local gradients. The measured in-plane displacements for similar stress regions agreed within 0.1 microns or better. Beyond the peak values, sinusoidal variations in amplitude compared well to both alternatively measured (holographically) and theoretically computed values.

However, end user test setups are often proprietary, so the results, while excellent, cannot be released. The goal of this effort was to thoroughly validate the ARAMIS 3D image correlation system for a critical application and make these results available to the testing and modeling communities at large.

EXPERIMENTAL PROCEDURE

The modeling and ballistic impact test program required for Return to Flight was not routine. It demanded ongoing innovation and state of the art facilities and techniques [6,7]. Gun barrel design, sabots, ice projectile fabrication, storage and handling, and precision aiming methods are just a few elements that were iterated together with the LS-DYNA code.

A prepared leading edge is shown in Figure 1 and the full-scale leading edge panel 9 test setup is shown in Figure 2 below. The pressure vessel and much of the gun barrel are out of sight. Important items to note are the reinforced carbon-carbon panels that are mounted to an orbiter wing leading edge section on a massive test stand. The 3D image correlation system camera bar is shown in Figure 3, and the reinforced first-surface mirror on its sine plate inside the leading edge is visible in Figure 4. The accident investigation took place at an outdoor full-scale test range at Southwest Research Institute, as shown in Figure 5; initial image correlation feasibility tests were also performed at this range. [8]

The use of the mirror was the subject of considerable discussion and checkout testing. Several checkout tests that verified removal of rigid body motion, including mirror tilting, are described elsewhere [9]. The success of the leading edge lab test and excellent matching between LS-DYNA and 3D image correlation for RCC coupon samples formed the basis for committing to 3D image correlation as the primary validation tool for full-scale leading edge tests. However, there was a need to verify that the ARAMIS 3D image correlation data would be accurate to within 5% of maximum peak displacement for any given test.

For these leading edge tests, it was determined that the primary deformation of interest peaked and recovered before the onset of relative rigid body motions that would require correction. Therefore, the movement correction algorithm software function in Aramis was not applied to any data for the full-scale tests.

For all validation tests, the actual systems in daily use at NASA Glenn and Southwest Research Institute were used, in the same lab or field conditions where testing was normally performed. Identical software settings were used as for the coupon and full-scale tests, which themselves were required to have identical settings for comparison purposes. The field of view was 14”, using 14 mm Nikon lenses at a working distance of approximately 30”. The image correlation facet (subset) size was 11 pixels, with a step between adjacent facets of 5 pixels. Two runs of a 5 x 5 facet matrix median filter were applied to displacements, and three runs of a 7 x 7 matrix median filter were applied to strains. For all impact tests, the Phantom v7 cameras were run at 27,000 frames per second with 256 x 256 active pixels. For the dynamic strain validation tests, the camera speed was reduced to 12,800 frames per second to match the data acquisition system sampling rate for strain gauges. The expected and verified out-of-plane displacement noise floor was approximately 50 microns (0.002”), and the strain noise floor was approximately 200-400 microstrain.

Figure 6 is a typical image correlation result from a ballistic impact on an Orbiter wing leading edge. Each section line shows the out-of-plane displacement profile along the impact trajectory, with 38.5 microseconds between lines on the plot. Many other types of analysis and presentation were performed, including overlays of time histories at impact and maximum displacement locations, and study of principal, longitudinal and transverse strains. However, the main quantity of interest was maximum displacement evolution over time, as indicated in this figure. The main purpose of this validation study was to provide absolute confidence about the accuracy of results such as these.

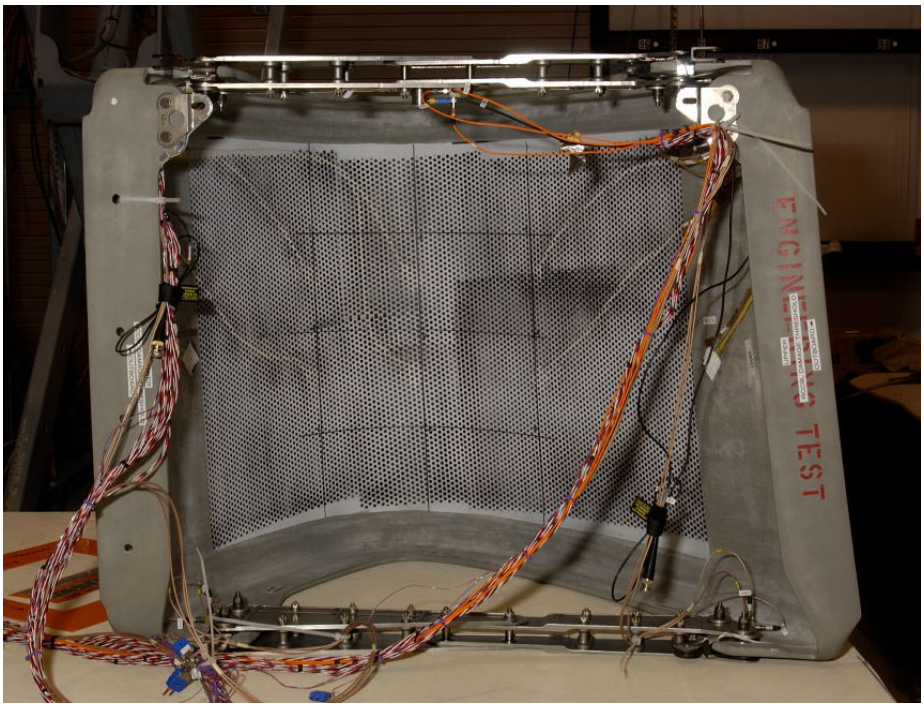

Figure 1: Orbiter wing leading edge reinforced carbon-carbon (RCC) engineering test article with dot pattern for image correlation applied, including fiducial marks at planned impact locations. Strain gauges and lead wires are visible as white outlines.

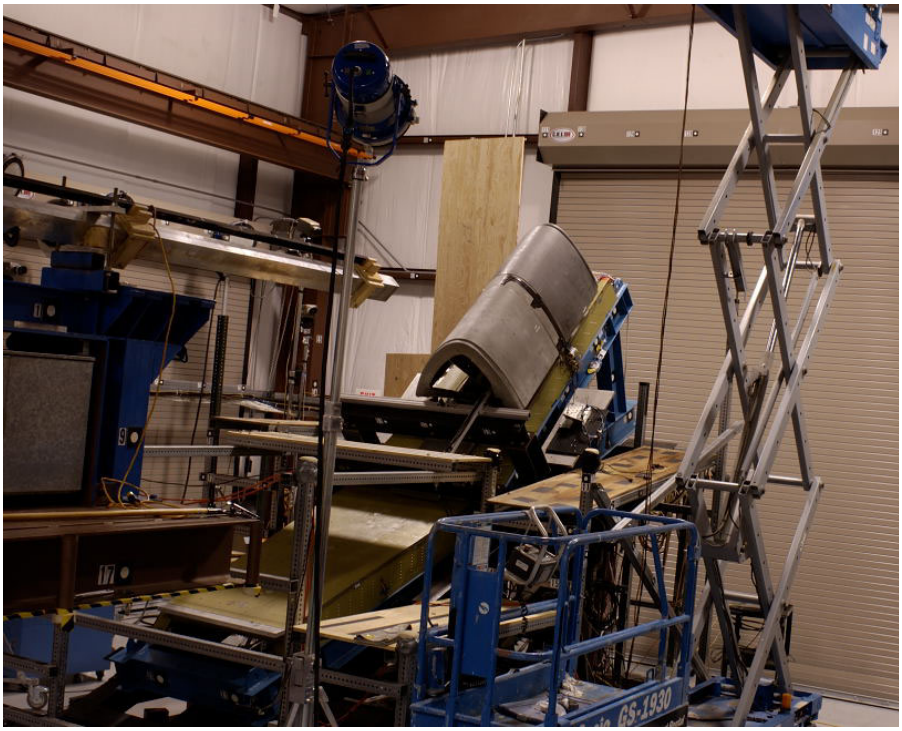

Figure 2: Wide angle view of ballistic impact setup for Orbiter leading edge panel 9 test series. RCC panels are mounted to wing leading edge on a massive test stand. The rectangular aluminum gun barrel extends towards the left edge of the photo.

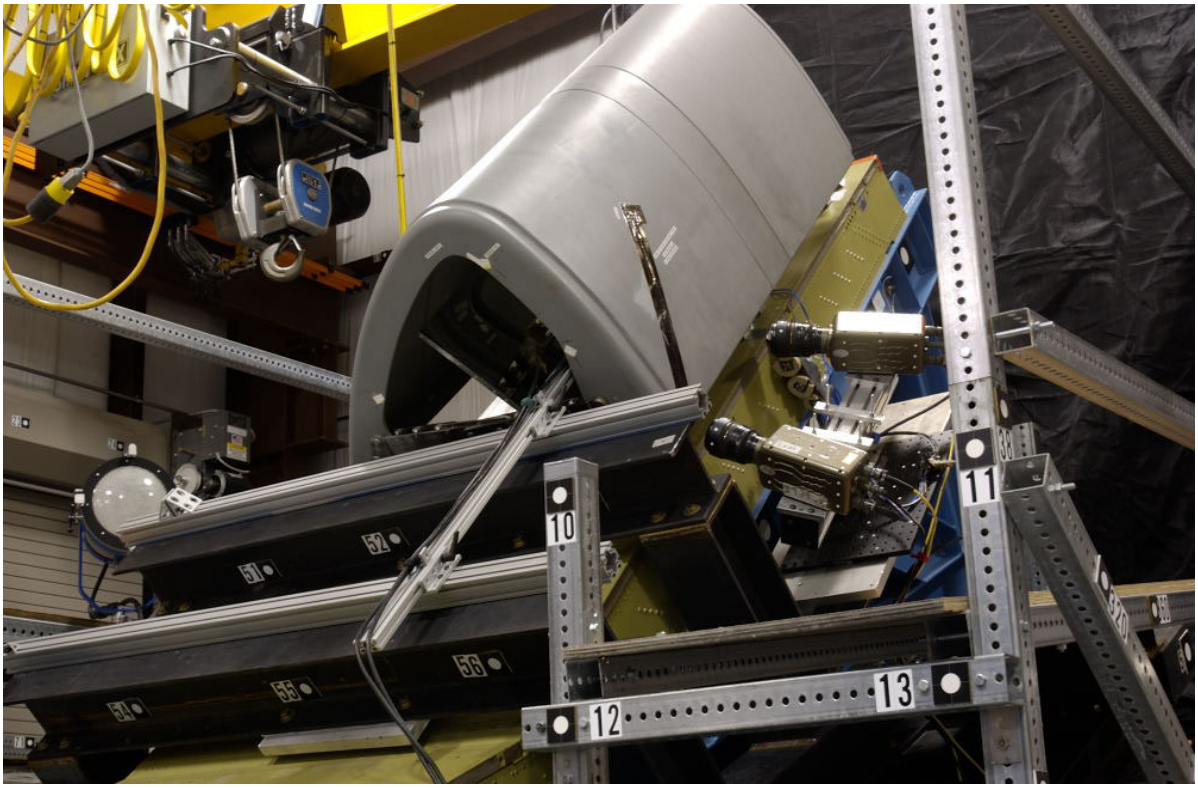

Figure 3: Close-up view of Phantom v7 camera pair on an adjustable sine plate, viewing through closeout panel gap. The entire camera bar can be moved to the opposite side of the test stand, to facilitate viewing the upper and lower surfaces as well as the apex area.

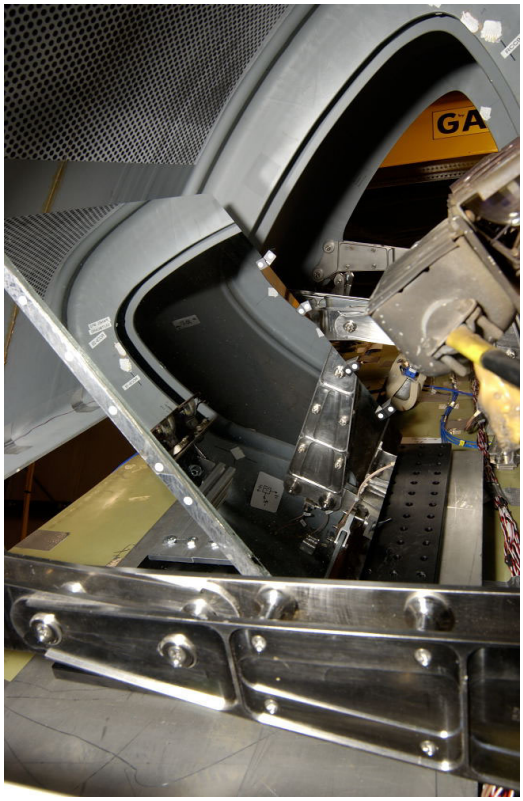

Figure 4: Reinforced first-surface mirror on an adjustable sine plate inside the RCC leading edge.

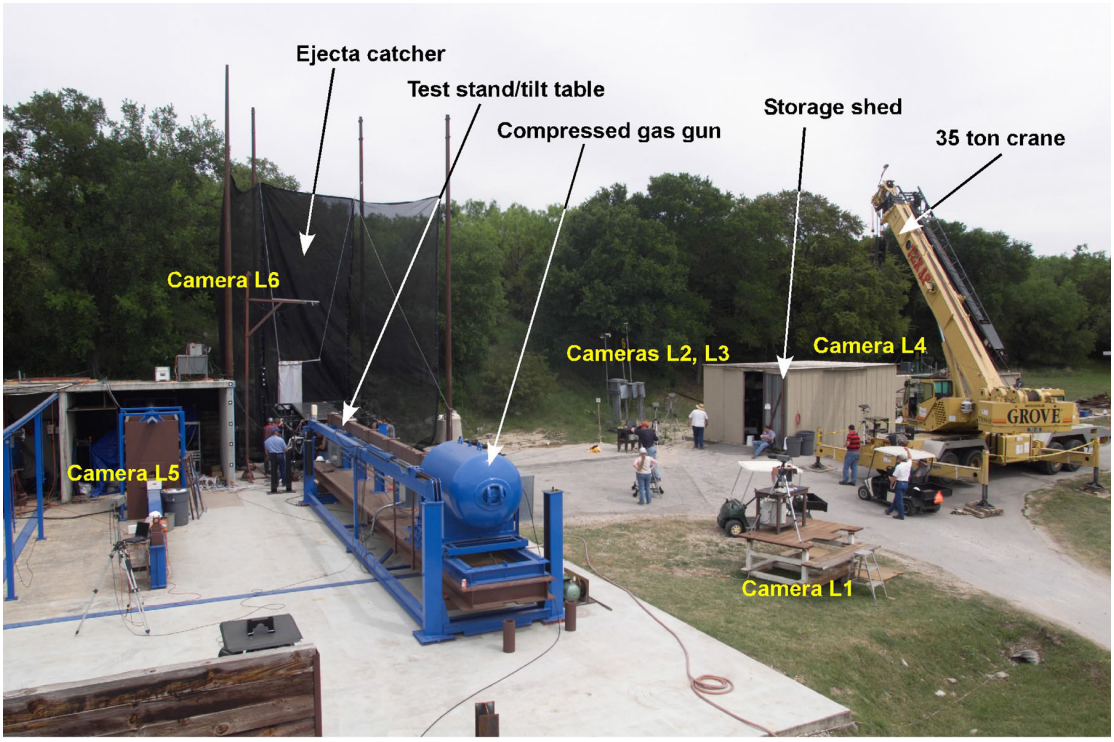

Figure 5: The outdoor full-scale test range at Southwest Research Institute where the accident investigation tests took place. Initial image correlation feasibility studies also occurred here.

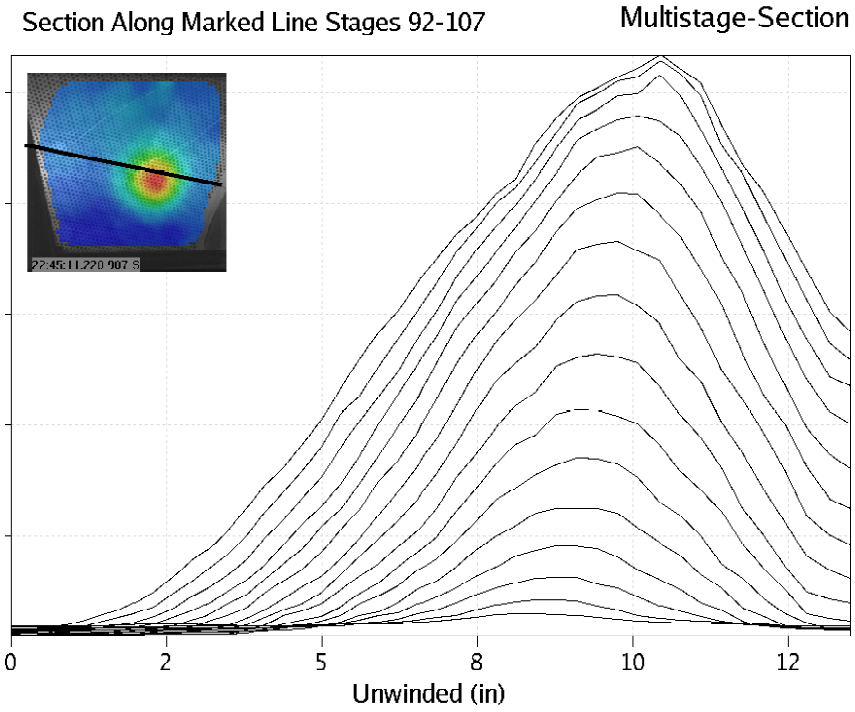

Figure 6: A typical result from the Aramis image correlation system for a leading edge foam impact shot. The section lines profile out-of-plane displacement along the impact trajectory, with 38.5 microseconds between each line on the chart. Absolute values have been removed because impact investigation tests are ongoing.

Static Rigid Body Panel Movements

The first quantitative verification test involved translating a flat panel relative to the camera bar in 0.1" increments up to a maximum of 1.0". Nominal values were determined using a calibrated digital caliper that had an accuracy of 0.1%.

Initially, the average value of out-of-plane deformation was compared to the nominal value read out from the micrometer. It was found that all values matched within 2%. However, it was noted that the error increased as the displacement increased. One explanation for this would be a systematic error such as a tilt of the panel. It was observed that the maximum deformation always occurred on the left edge of the panel. Comparison of the maximum value read out for the same point to the nominal value resulted in significantly lower errors, as shown in Table 1, and eliminated the trend of increasing error as displacement increased.

Table 1: Nominal and Measured Panel Displacements (Inches) and Errors

Nominal Displacement	Aramis Minimum	Aramis Maximum	Aramis Average	Error in Average	Error in Maximum
0.1	0.09567	0.09957	0.09696	0.304%	0.04%
0.2	0.1922	0.1978	0.19368	0.632%	0.22%
0.3	0.2876	0.2956	0.2903	0.970%	0.44%
0.4	0.3854	0.3982	0.38809	1.191%	0.18%
0.5	0.4827	0.4893	0.48579	1.421%	1.07%
0.6	0.578	0.5927	0.58499	1.501%	0.73%
0.7	0.679	0.696	0.68463	1.537%	0.40%
0.8	0.775	0.792	0.78137	1.863%	0.80%
0.9	0.873	0.8891	0.88052	1.948%	1.09%
1	0.9717	0.9908	0.98002	1.998%	0.92%

Laboratory Verification of Dynamic Displacement and Strains

In order to verify dynamic displacements, several tests were conducted at the NASA Glenn Ballistic Impact Laboratory, where several hundred RCC and external tank coupon panel ballistic impact tests were also performed. An aluminum plate was prepared with a dot pattern and held in a vise for one test and attached to a shaker for another. The Phantom v7 camera bar imaged the panel, as shown in Figure 7. The panel was also instrumented with accelerometers and strain gauges, and a pair of Keyence model 2450 laser displacement gauges, as shown in Figure 8. The Keyence sensors were calibrated against a precision micrometer measuring rigid body translation of the panel, similar to the static tests described above. The strain gauges were calibrated by loading the plate with a weight and compared to calculated strain values. A further verification of the Keyence sensors was made by mounting the plate on a Bruel and Kjaer shaker and inducing known displacements at various frequencies.

The initial finding was that the 3D image correlation data matched the laser sensor and strain gauge data with a 12% worst-case error for displacement and 9% worst-case error for strain. Average error over the entire time history was lower than this. Nevertheless, because of the unexpectedly poor match, all aspects of the test setup and data reduction were closely examined. It was found that there was a very strong gradient, especially for displacements but also for strains, in the vicinity of the gauges. The gauges had been located relatively close to the root of the cantilever plate in order to get sufficiently high bending strains and sufficiently low displacements. In fact, there was a 13.6% change in displacement between two adjacent facets (image correlation data points) in the vertical direction.

Once this was understood, linear interpolation was used to read out the image correlation data at the exact gauge locations, which were between available data points. This was done by hand for the first case, and then a Matlab script was used to automate the process and create time histories with up to 1500 time sample points for each test. The spatial resolution for the interpolation was 0.075". The exact same distance from the edge of the plate to the readout location was used for each test. The final results of the comparison are shown in Table 2 below. It can be seen that the worst-case difference for displacement was only 1.27%. The strain difference increased as strain decreased towards the noise floor of the image correlation system, which is expected. Strains from the ballistic impacts were well above the noise floor, and, more importantly, the displacement data was used for validating the DYNA models, instead of strains.

The validation test setups and results, including comparison to calculated values, will be more thoroughly reported in the future.

Table 2: Final Results of Laboratory Dynamic Validation Test

Laser Displacement (In)	Aramis Displacement (In)	Displacement Difference (%)	Gauge Strain (με)	Aramis Strain (με)	Strain Difference (%)
0.3635	0.3638	**0.08**	2034	2060	**1.28**
0.2432	0.2452	**0.82**	1358	1365	**0.52**
0.1855	0.1876	**1.13**	1067	1027	**-3.75**
0.1043	0.1036	**-0.67**	607	575	**-5.27**
0.0632	0.0624	**-1.27**	354	381	**7.63**

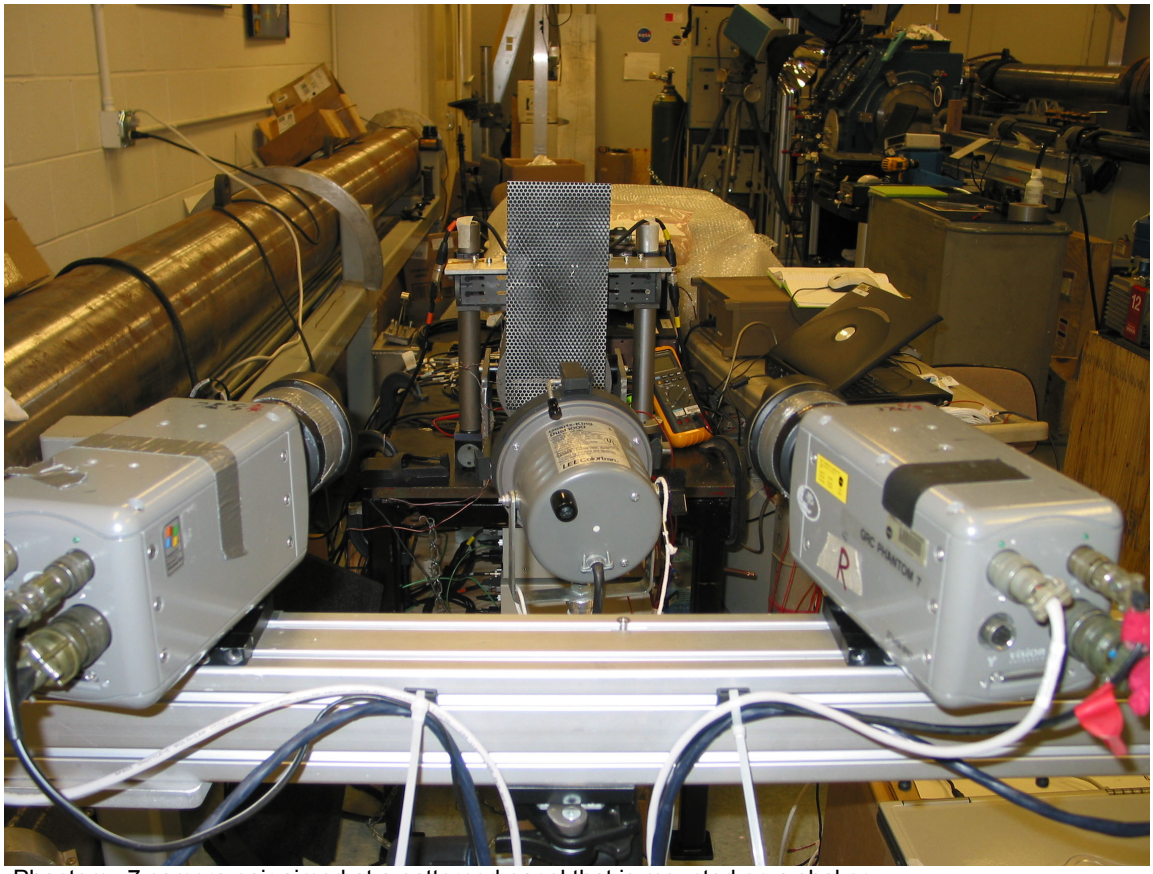

Figure 7: Phantom v7 camera pair aimed at a patterned panel that is mounted on a shaker.

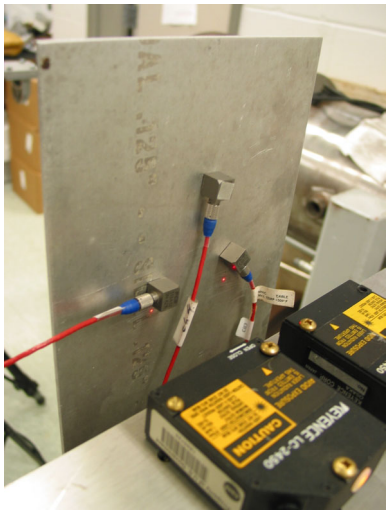

Figure 8: Rear side of panel showing accelerometers and laser displacement sensors. Strain gauges are mounted on the front face.

Field Comparison of Dynamic Strains From Ballistic Impact

Because the impact investigation and modeling effort is still ongoing, full details of the strain comparisons, such as time histories, cannot yet be released. However, the comparison method and one quantitative example can be shown. Figure 9 shows a full-field plot from the 3D image correlation system of principal strain at the moment of maximum amplitude during an impact event. The black outline is the location of a strain rosette, though the gauge actually occupied only about 2/3 of the delineated area. Note that there is a high strain gradient at the gauge, as well as a much higher peak strain a short distance away, of which the strain gauge would have no knowledge. Image correlation data was read out from discrete virtual gauge points at the left, middle and right of the bonded strain gauge. In this case, the values were 2100, 2400 and 2700 microstrain respectively, while the strain gauge indicated 2100 microstrain. Time history shapes and lateral to longitudinal strain values and ratios were also compared with satisfactory results, for multiple impact events, sometimes for multiple gauges within the field of view.

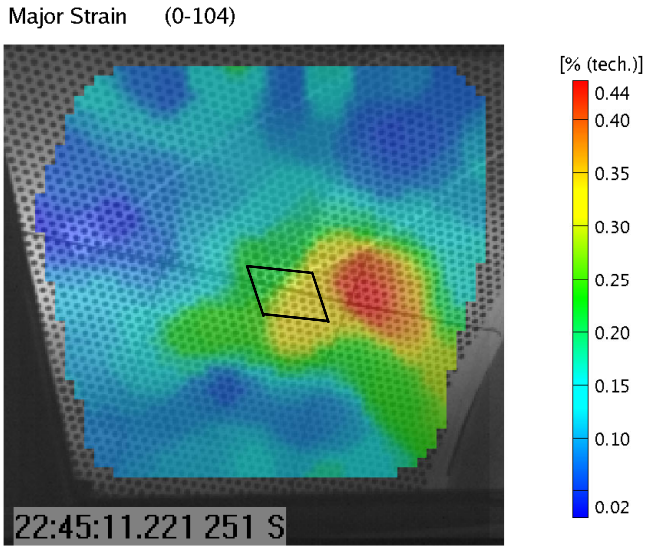

Figure 9: Image correlation full-field principal strain map with strain gauge location indicated by black outline. Note that there is a gradient across the gauge area, and that there is a much higher peak strain area a short distance away, of which the strain gauge would have no knowledge.

CONCLUSIONS

The accuracy of the ARAMIS 3D image correlation system with Phantom v7 high-speed digital cameras was thoroughly investigated in both field and laboratory conditions. Rigid body panel translation results conducted in-situ on a test range matched a calibrated micrometer within 1.09% for 0.1" increments from 0.1 to 1.0 inches, with much greater accuracy for most increments. Dynamic displacements from a bend and release test in a laboratory closely matched those from a laser interferometer, and strains from the same test matched both strain gauges and calculated values. The worst-case error for dynamic displacement was 1.27%. In addition, dynamic strains reported during critical Return to Flight Orbiter leading edge panel impact tests were repeatedly found to satisfactorily match data from strain gauges within the field of view.

3D image correlation using digital high-speed cameras has been shown to be an invaluable tool, now in everyday use for critical ballistic impact investigations. The technique is also broadly applicable for air blast deformation measurements, crash testing, high strain rate testing, and other dynamic phenomena. Dynamic displacement data forms the basis for validation and iteration of LS-DYNA models. Full-field strain data reveals strain gradients. Measurements have been performed in adverse field conditions, including extreme heat and cold, inside and through vacuum chambers, and in close proximity to high explosives.

Objective validation efforts are critical for the acceptance of relatively new measurement systems such as 3D image correlation. Developers, application engineers and end users are encouraged to disseminate objective studies of the applicability and accuracy of 3D image correlation.

ACKNOWLEDGMENTS

This paper incorporates the efforts of numerous individuals working tirelessly on the NASA Return to Flight program.

Justin Kerr of NASA Johnson provided superb leadership for the full-scale test team at Southwest Research Institute, San Antonio, Texas. Ovidio Oliveras was the main 3D image correlation system operator, and provided timely reports despite an otherwise full workload. Jay Laughman gave mechanical and moral support, and was also responsible for weekly poker games. The value of these games for morale was incalculable; the cost for a beginner could be high.

Don Grosch and Freeman Bertrand designed and fabricated the image correlation support structure on the test stand for the full-scale leading edge impact tests.

We thank Ed Oshel for sharing his expert knowledge of photogrammetry with other members of the test team. His detailed explanations of both the theoretical and practical aspects of intersection errors were particularly valuable.

People provide more important support for digital high-speed cameras than tripods do. We are grateful for exceptional help from many individuals at Vision Research, especially Bill Shipman, Ed Julian, Tim Mills and Andy Kubit.

Sergey Samorezov designed the dynamic validation test at NASA Glenn and calibrated the Keyence sensor, accelerometers and strain gauges.

Matt Crandall of Lockheed Martin produced software tools to simplify calibration and image import.

Kelly Carney of NASA Glenn discussed the general challenges of modeling and its validation, particularly for complex materials such as reinforced carbon-carbon.

Jerry Bohr, Boeing Technical Fellow, rigorously reviewed 3D image correlation principles in addition to making detailed comparisons to strain gauges that he was responsible for. He also oversaw tap hammer testing of the image correlation setup.

Philip Kopfinger and Jimmy Blevins of Lockheed Martin oversaw the first rigorous validation testing of high-speed 3D image correlation for ballistic impact work, on highly instrumented external tank coupon samples.

All of the image correlation results were processed using GOM ARAMIS version 5.3 or 5.4 software.

REFERENCES

1. Gehman, H.W. et al, Columbia Accident Investigation Board Report, Volume 1, US Government Printing Office, Washington, DC, August 2003.

2. NASA's Implementation Plan for Space Shuttle Return to Flight and Beyond, Volume 1, Ninth Edition, March 18, 2005.

3. Schmidt, Tyson and Galanulis, Full-Field Dynamic Displacement and Strain Measurement Using Advanced 3D Image Correlation Photogrammetry, Experimental Techniques, Part I: May/June 2003, Vol. 27 #3, p.47-50, Part II: July/Aug, Vol. 27 #4, p.44-47.

4. Z.L. Kahn-Jetter and T.C. Chu, Three-dimensional Displacement Measurements Using Digital Image Correlation and Photogrammetric Analysis, Experimental Mechanics, Vol. 30, No. 1, pp. 10-16, March 1990.

5. Nelson, Makino and Schmidt, Residual Stress Determination Using Hole Drilling and 3D Image Correlation, Proceedings of the 2005 SEM Annual Conference and Exposition, Portland, Oregon, June 7-9, 2005.

6. J. Michael Pereira, Matthew E. Melis, and Duane M. Revilock, A Summary of the Space Shuttle Columbia Tragedy and the Use of Digital High Speed Photography in the Accident Investigation and NASA's Return-to-Flight Effort, SPIE 26th ICHSPP, September 2004.

7. Melis, Carney et al, A Summary of the Space Shuttle Columbia Tragedy and the Use of LS DYNA in the Accident Investigation and Return to Flight Efforts, 8th International LS-DYNA Users Conference, Dearborn, Michigan, May 2-4, 2004.

8. Schmidt, Tyson, Galanulis, Revilock and Melis, Full-field dynamic deformation and strain measurements using high-speed digital cameras, Proceedings of the SPIE 26th International Congress on High-Speed Photography and Photonics, Alexandria, VA, Sept 19, 2004.

9. Schmidt, Tyson and Galanulis, 3D Image Correlation Using Digital High Speed Cameras: Results and Considerations, Proceedings of the 2005 SEM Conference and Exposition, Portland OR, June 7-9, 2005.